ApJ, accepted April 28, 2006

# SDSS J1534+1615AB: A Novel T Dwarf Binary Found with Keck Laser Guide Star Adaptive Optics and the Potential Role of Binarity in the L/T Transition[1]

Michael C. Liu,[2,3] S. K. Leggett,[4] David A. Golimowski,[5]
Kuenley Chiu,[5] Xiaohui Fan,[6] T. R. Geballe,[7] Donald P. Schneider,[8] J. Brinkmann[9]

## ABSTRACT

We have resolved the newly discovered T dwarf SDSS J153417.05+161546.1 into a $0.11''$ binary using the Keck sodium laser guide star adaptive optics system. With an integrated-light near-IR spectral type of T3.5±0.5, this binary provides a new benchmark for studying the distinctive $J$-band brightening previously noted among early and mid-T dwarfs, using two brown dwarfs with different spectral types but having a common metallicity and age and very similar surface gravities. We estimate spectral types of T1.5±0.5 and T5.5±0.5 for the two components based on their near-IR colors, consistent with modeling the integrated-light spectrum as the blend of two components. The observed near-IR flux ratios of SDSS J1534+1615 are unique compared to all previously known substellar binaries: the component that is fainter at $H$ and $K'$ is brighter at $J$. This inversion of the near-IR fluxes is a manifestation of the $J$-band brightening within this individual binary system. Therefore, SDSS J1534+1615 demonstrates that the brightening can be intrinsic to ultracool photospheres (e.g., arising from cloud disruption and/or rapid increase in cloud sedimentation) and does not necessarily result from physical variations among the observed ensemble of T dwarfs (e.g., a range in

[1]The data presented herein were obtained at the W.M. Keck Observatory, which is operated as a scientific partnership among the California Institute of Technology, the University of California, and the National Aeronautics and Space Administration. The Observatory was made possible by the generous financial support of the W.M. Keck Foundation.

[2]Institute for Astronomy, University of Hawai'i, 2680 Woodlawn Drive, Honolulu, HI 96822; mliu@ifa.hawaii.edu

[3]Alfred P. Sloan Research Fellow

[4]United Kingdom Infrared Telescope, Joint Astronomy Centre, 660 North A'ohoku Place, Hilo, HI 96720

[5]Department of Physics and Astronomy, Johns Hopkins University, 3400 North Charles Street, Baltimore, MD 21218-2686

[6]Steward Observatory, University of Arizona, 933 North Cherry Avenue, Tucson, AZ 85721

[7]Gemini Observatory, 670 North A'ohoku Place, Hilo, HI 96720

[8]Department of Astronomy and Astrophysics, Pennsylvania State University, University Park, PA 16802

[9]Apache Point Observatory, 2001 Apache Point Road, P.O. Box 59, Sunspot, NM 88349

masses, ages and/or metallicities). We suggest that the apparently large amplitude of the $J$-band brightening may be due to a high incidence of unresolved binaries and that the true amplitude of the brightening phenomenon could be more modest. This scenario would imply that truly single objects in these spectral subclasses are relatively rare, in agreement with the small effective temperature range inferred for the L/T transition.

*Subject headings:* binaries: general, close — stars: brown dwarfs — stars: atmospheres — infrared: stars — techniques: high angular resolution

## 1. Introduction

For many decades, color-magnitude diagrams (CMDs) have provided fundamental insights into the physics of stellar evolution and stellar atmospheres. In an analogous fashion, the CMDs of brown dwarfs are beginning to shed light on the physical properties of these low mass objects, as an increasing number of distances have been determined from trigonometric parallaxes for field brown dwarfs (Dahn et al. 2002; Tinney et al. 2003; Thorstensen & Kirkpatrick 2003; Vrba et al. 2004) and from brown dwarf companions around stars with known distances (e.g. Becklin & Zuckerman 1988; Nakajima et al. 1995; Rebolo et al. 1998; Burgasser et al. 2000; Kirkpatrick et al. 2001; Liu et al. 2002; Potter et al. 2002; Freed et al. 2003; Metchev & Hillenbrand 2004).

However, interpretation of brown dwarf CMDs is considerably less developed than for the case of stellar CMDs. Brown dwarfs continually cool as they age, unlike stars which occupy a fixed position on the CMD during the main-sequence phase. Therefore, there are degeneracies in determining the masses and ages of brown dwarfs from the CMD. Substellar photospheres have a rich appearance due to the presence of dust and molecules (e.g., metal hydrides, water vapor, and methane), and spectroscopic methods to determine the associated physical properties, such as effective temperature and surface gravity, are still under development (e.g. Kirkpatrick 2005). The optical and infrared CMDs of brown dwarfs show considerable scatter which could be due to differences in metallicity, surface gravity (i.e., mass), rotation, dust properties, and/or unrecognized binarity among the observational ensemble (e.g. Leggett et al. 2002; Knapp et al. 2004).

Study of ultracool binary systems is a promising means to address these issues, since binaries provide systems with common ages and metallicities. About two dozen L dwarf binaries are now known from high resolution imaging of over a hundred L dwarfs, mostly by *HST* (Koerner et al. 1999; Martín et al. 1999; Reid et al. 2001; Gizis et al. 2003; Bouy et al. 2003; Golimowski et al. 2004b). In contrast, only five ultracool binaries that include at least one T dwarf have been identified: 2MASS J1225−2739AB (T6+T8; Burgasser et al. 2003b), 2MASS J1534−2952AB (T5.5+T5.5; Burgasser et al. 2003b), $\epsilon$ Ind Bab (T1+T6; McCaughrean et al. 2004), SDSS J0423−0414AB (L6+T2; Burgasser et al. 2006), and 2MASS J2252−1730AB (L6+T2; Reid et al. 2006).[1] Un-

[1]Some other objects are suspected of being L+T binaries, i.e., systems composed of an L dwarf and a T dwarf,

derstanding the transition between objects of spectral type L, marked by very red IR colors and metal hydride absorption, and those of spectral type T, marked by blue IR colors and methane absorption, has been an active area of inquiry (e.g. Leggett et al. 2004). An expanded sample of L-type and T-type binaries should shed light on this issue.

We are conducting an imaging survey of nearby brown dwarfs using the new Keck laser guide star adaptive optics system (LGS AO). LGS AO enables near diffraction-limited imaging over most of the sky with a 10-meter telescope. Thus, LGS AO is a powerful new capability for finding and characterizing substellar binaries. We have previously used Keck LGS AO to discover that the nearby L dwarf Kelu-1 is a binary system (Liu & Leggett 2005), thereby explaining the unusual properties of Kelu-1 (high luminosity, very red color, high inferred effective temperature, and low lithium absorption line strength) compared to other early L dwarfs. In this paper, we present the discovery of the binarity of SDSS J153417.05+161546.1 (hereinafter SDSS J1534+1615), a recently discovered T dwarf with an integrated-light near-IR spectral type of T3.5±0.5 (Chiu et al. 2006), and consider the implications for understanding the L/T transition.

## 2. Observations

We observed SDSS J1534+1615 on 2005 May 1 UT using the sodium LGS AO system (Bouchez et al. 2004; Wizinowich et al. 2004) of the 10-meter Keck II Telescope on Mauna Kea, Hawaii. We used the facility IR camera NIRC2 and the $J$ (1.25 $\mu$m), $H$ (1.64 $\mu$m), and $K'$ (2.12 $\mu$m) filters from the Mauna Kea Observatories (MKO) filter consortium (Simons & Tokunaga 2002; Tokunaga et al. 2002). We used NIRC2's narrow camera, which produces a 0.00994″ pixel$^{-1}$ scale and a 10.2″ field of view. Conditions were photometric with excellent seeing conditions during the night, better than 0.6″ in the optical as reported by the neighboring Keck I Telescope. The total setup time for the telescope to slew to SDSS J1534+1615 and for the LGS AO system to be fully operational was 18 minutes. SDSS J1534+1615 was observed over an airmass range of 1.14–1.24.

The LGS brightness, as measured by the flux incident on the AO wavefront sensor, was equivalent to a $V \approx 10.3$ mag star. The LGS provided the wavefront reference source for AO correction, with the exception of tip-tilt motion. Tip-tilt aberrations and quasi-static changes in the image of the LGS as seen by the wavefront sensor were sensed using the $R = 15.9$ mag star 1062-0236346 from the USNO-B1.0 catalog (Monet et al. 2003), located 14″ away from SDSS J1534+1615. The overall image quality was somewhat worse compared to other data obtained on the same night (Liu & Leggett 2005) due to higher winds during the SDSS J1534+1615 observations. The LGS AO-corrected images have full widths at half maxima (FWHM) of 0.08″, 0.06″, and 0.07″ at $JHK'$, respectively, with RMS variations of about 5–10%. The corresponding Strehl ratios were 0.02, 0.06,

based on their resolved optical data (2MASS J0850+1057 [Reid et al. 2001] and 2MASS J1728+3948 [Gizis et al. 2003]), near-IR flux ratios (Gl 337CD; Burgasser et al. 2005b), or integrated-light spectra (2MASS J0518−2828 [Cruz et al. 2004] and 2MASS J0920+3517 [Reid et al. 2001; Nakajima et al. 2001; Burgasser et al. 2005a]).

and 0.20 with RMS variations of about 5–20%. The FWHM and Strehl measurements were derived from the result of the binary fitting process described below.

We obtained a series of five images in each filter, dithering the telescope by a few arcseconds between each image. The total on-source integration time per filter was 7.5 minutes. The sodium laser beam was steered with each dither such that the LGS remained on SDSS J1534+1615 for all exposures. This object was easily resolved into a binary system in all our data. The images were reduced in a standard fashion. We constructed flat fields from the differences of images of the telescope dome interior with and without lamp illumination. Then we created a master sky frame from the median average of the bias-subtracted, flat-fielded images and subtracted it from the individual images. Images were registered and stacked to form a final mosaic (Figure 1). The known small geometric distortions in NIRC2 have a negligible effect on our analysis.

To measure the flux ratios and relative positions of the two components, we adopted two methods. (1) The first method used an analytic model of the point spread function (PSF) as the sum of two elliptical Gaussian components, a narrow component for the PSF core and a broad component for the PSF halo. (2) The second method empirically determined the PSF using the Starfinder software package (Diolaiti et al. 2000), which was designed for analysis of blended AO images. For the individual images obtained with each filter, we fitted for the flux ratio, separation, and position angle of the binary. The averages of the results were adopted as the final measurements and the standard deviations as the errors. The results from the two different methods were generally consistent.

In order to gauge the accuracy of these two measurement methods, we created artificial binary stars from data of single stars that had comparable image quality (similar tiptilt star properties, Strehl ratios, and FWHM) to the SDSS J1534+1615 data. Our two methods were applied to the artificial binaries to assess the fitting results and derived errors. Based on this analysis, we adopted the Starfinder measurements for the $H$-band and $K'$-band data, and the Gaussian fitting results for the $J$-band data. These choices were not unexpected: the higher Strehl, long wavelength data had a more structured PSF which was better treated by Starfinder, while the much smoother, low Strehl $J$-band images were modeled better by the two-gaussian PSF. Table 1 presents the resulting flux ratios and astrometry results.

Table 2 reports the IR apparent magnitudes and colors of the individual components, as derived from our flux ratio measurements and the integrated IR magnitudes reported by Chiu et al. (2006). The absolute magnitudes for SDSS J1534+1615 are unknown, as a trigonometric parallax is not available for this system. Also, in principle variability could impact the photometry determined for the individual components, since the integrated-light photometry was obtained at a different epoch than the Keck LGS AO measurements of the flux ratios. IR monitoring of a limited number of T dwarfs does find low-level variability in some objects, though the timescales and persistence are not well-constrained (Enoch et al. 2003; Koen et al. 2004, 2005). SDSS J1534+1615 has been observed at 4 epochs by the SDSS survey over a span of 11 months and shows no $z$-band (0.9 $\mu$m)

variability at the ∼0.1 mag level.

Our NIRC2 $J$ and $H$-band imaging used the same MKO filters as Chiu et al. (2006) and hence computing magnitudes for the individual components from our measured flux ratios is straightforward. However, our NIRC2 data were obtained with the MKO $K'$-band (2.12 $\mu$m) filter in order to minimize the thermal background from the sky + AO system, whereas the Chiu et al. photometry used the MKO $K$-band (2.20 $\mu$m) filter. Liu & Leggett (2005) reported a polynomial fit for the $(K'-K)_{MKO}$ color term as a function of spectral type for L and T dwarfs using synthetic photometry based on the data from Knapp et al. (2004). However, for the range of spectral types relevant to SDSS J1534+1615 (see § 3), the color term depends strongly on the spectral type inferred from the $J-H$ color. Instead, we use the synthetic photometry to find a direct relation for the color term as a function of the $J-H$ color:

$$(K'-K)_{MKO} = -0.100 + 0.143 \times (J-H)_{MKO}, \quad (1)$$

valid for L and T dwarfs with $-0.5 < (J-H) < 1.0$. The resulting $(K'-K)$ terms are 0.02 and $-0.13$ mags for components A and B, respectively. The RMS scatter about the fit is 0.03 mags, which we add in quadrature when determining the $K$-band photometry errors of the individual components.

Figure 1 shows the unique behavior of the near-IR flux ratios for SDSS J1534+1615AB compared to all other known substellar binaries: namely, the identification of the brighter component depends on the observing wavelength. We designate the eastern object as the "A" component, based on the fact that its inferred spectral type is earlier than the western component, as discussed in § 3. The eastern object is brighter in $H$ and $K'$ bands, and we would also expect it to be the brighter component at optical wavelengths, based on the T dwarfs with known distances (Tinney et al. 2003). The western, later-type object is brighter only in the $J$-band images. This can be understood as a manifestation of the $J$-band brightening seen in the absolute magnitudes of T dwarfs, wherein objects of spectral types from about T2 to T5 are notably brighter at $J$-band compared to earlier type objects (Dahn et al. 2002; Tinney et al. 2003; Vrba et al. 2004). We discuss this further in § 4.

No other sources are detected in our images. For objects at $\gtrsim$0.3″ from SDSS J1534+1615, the final mosaics reached point source detection limits of 21.0, 21.0, and 20.7 mags at $JHK'$, respectively, out to a separation of 3″. For an age range of 0.5–5 Gyr and a estimated distance of 36 pc (see § 3), these detection limits correspond to about 10–30 $M_{Jup}$ companions around SDSS J1534+1615 based on the models of Baraffe et al. (2003).

## 3. Results: Properties of SDSS J1534+1615AB

With only one epoch of imaging, we cannot ascertain whether the two objects in our Keck images are physically associated based solely on common proper motion. However, the combination

of the small proper motion and the distinctive optical/IR colors can only be explained if the system is a binary T dwarf. No relative motion was detected between the two components during the 30 minutes elapsed time for the Keck LGS AO imaging, so component B cannot be a solar system body (which would be expected to show a relative motion of $\gtrsim$0.5″). SDSS J1534+1615 was detected at $J$ and $H$-bands by 2MASS in 1999 and by SDSS in both 2004 and 2005, giving a proper motion of 0.15″/yr at position angle 248° east of north. The small proper motion indicates that the optical and IR photometry in Chiu et al. (2006) represents the combined light of both objects, and thus our Keck IR flux ratio measurements can be used to derive the resolved photometry of the individual components. The resulting IR colors for the two components are entirely consistent with those of T dwarfs. Component B does have neutral $JHK$ colors similar to hot O stars and white dwarfs, but if it were either of these objects, the integrated optical light of the system would be predominantly blue rather than very red as observed ($z - J = 3.61 \pm 0.10$ mags; Chiu et al. 2006). Hence, we conclude that the two objects constitute a binary T dwarf.

To infer spectral types, we compare the resolved $JHK$ colors of SDSS J1534+1615AB to those of ultracool dwarfs from Knapp et al. (2004) and Chiu et al. (2006), excluding any known binaries. Our measurements and the published photometry were both obtained with the MKO filter system. For the L dwarfs, we use the published spectral types, which are based on the Geballe et al. (2002) near-IR classification scheme. For the T dwarfs, we use near-IR classfications from the Burgasser et al. (2005a) scheme. (We adopt these two classification schemes throughout this paper, which includes updating older published T dwarf types to the new Burgasser et al. scheme.) We assume that the components of SDSS J1534+1615 are themselves single, not unresolved binaries. Figure 2 shows that component A has IR colors most typical of the known T1 dwarfs, with T2 also being possible. (The colors of component A are also similar to the few late-L dwarfs with unusually blue near-IR colors in Figure 2. However, as discussed below, modeling of the integrated-light spectrum indicates that this is unlikely.) Component B has IR colors most similar to the T5 dwarfs and some of the T6 dwarfs. We estimate spectral type estimates of T1.5±0.5 and T5.5±0.5 for the two components.[2]

We modeled the integrated-light spectrum of SDSS J1534+1615 as the blend of two template T dwarfs, in order to check the consistency with the flux ratios and spectral types inferred from our Keck LGS imaging. For templates, we chose T dwarfs from Figure 2 with complete $JHK$ spectra and having similar near-IR colors to the two components of SDSS J1534+1615 (color differences of $\lesssim$0.1 mags). Then we scaled the template spectra to match the observed $J$-band flux ratio, summed the templates to form a composite spectrum, and scaled the resulting composite to the observed integrated-light spectrum. (Note that this approach has only one free parameter in the modeling, namely the distance to the binary.) The comparisons between the model composite spectra and

[2]We assume that the metallicity of SDSS J1534+1615 is not very different than the bulk of the known T dwarfs. The low proper motion argues against it being a halo object. Likewise, the one candidate low-metallicity T dwarf reported by Burgasser et al. 2003a is distinguished by an exceptionally blue $H - K$ color, whereas the colors of SDSS J1534+1615 are consistent with other T dwarfs.

the observed spectrum show good agreement (Figure 3).[3] Likewise, although SDSS J1534+1615A has near-IR colors similar to some of the bluest late-L dwarfs, it was not possible to create a well-matched composite spectrum with a blue late-L dwarf as a template, and thus we discount this possibility. Overall, the spectral types estimated from modeling the integrated-light spectrum agree well with those from the resolved Keck near-IR colors.

In the absence of a trigonometric parallax, the model composite spectra can provide a rough distance estimate for SDSS J1534+1615AB. The spectra were created using 2MASS J2356−1553 (T5.5; Burgasser et al. 2002b) and SDSS J2124+0100 (T5; Chiu et al. 2006) to represent component B. Vrba et al. (2004) have measured a trigonometric parallax for 2MASS J2356−1553. For SDSS J2124+0100, we assumed an absolute $J$-band magnitude of 14.37 mags, based on the polynomial fit for the absolute $J$-band magnitude as a function of spectral type from Knapp et al. (2004). Assuming these two mid-T templates are single objects, the inferred distance modulus for SDSS J1534+1615AB is 2.7–2.9 mags (≈36 pc). To check on the distance estimated from our spectral modeling, we applied the same procedure to the integrated-light spectrum of the binary T dwarf $\epsilon$ Ind Bab (McCaughrean et al. 2004) and derived a distance estimate of 3.3 pc, in good agreement with the measured distance of 3.626±0.009 pc (Perryman et al. 1997).

We can estimate the mass ratio SDSS J1534+1615AB, independent of its distance. For the assumed spectral types of T1.5±0.5 and T5.5±0.5, the difference in bolometric corrections for the two components is 0.55±0.15 mags, with $BC_K$ being larger for the T1.5±0.5 component (Golimowski et al. 2004a). The $K$-band flux ratio for the system is 1.21±0.05 mags, based on our Keck LGS images and the $(K' - K)$ color term calculated in § 2. Hence, the difference in bolometric luminosities is 0.7±0.2 mags, with component A having the higher luminosity. Burrows et al. (2001) provide an approximate mass-luminosity relation for coeval solar-metallicity brown dwarfs, $L_{bol} \propto M^{2.64}$. This implies a mass rataio of about 0.80±0.05 for the two components of SDSS J1534+1615, which is similar to the nearly equal mass ratios found for other binary brown dwarfs (e.g. Burgasser et al. 2003b).

Likewise, we can estimate the surface gravity difference for the two components, independent of the distance. Since the radii of brown dwarfs older than $\gtrsim$300 Myr are nearly independent of the masses, the near-unity mass ratio means that the surface gravities of SDSS J1534+1615A and B are very similar. Burrows et al. (2001) present analytic fits to substellar evolutionary models that show the quantity $g^{1.7}{T_{\rm eff}}^{-2.8}$ is constant at fixed age. Adopting $T_{\rm eff}$ ranges of ≈1300–1400 K and ≈1100–1200 K for components A and B, respectively (Golimowski et al. 2004a, which assumes an age of 3 Gyr), the inferred difference in surface gravities is approximately 0.05–0.15 dex.

[3]We also tried using T dwarfs with known distances as templates (as compiled in Knapp et al. 2004), directly summing the flux-calibrated spectra without imposing the $J$-band flux ratio. The resulting set of blended spectra could not simultaneously match the SDSS J1534+1615 integrated-light spectrum and the observed $JHK$ flux ratios. The mismatch is not surprising given that most of the T dwarfs with measured distances do not have the same near-IR colors as SDSS J1534+1615A and B. As Figure 2 shows, there is significant color scatter within a given T subclass.

We can make a rough estimate of the orbital period of SDSS J1534+1615AB, assuming that the true semi-major axis is not very different than the projected separation. (For example, Fischer & Marcy 1992 show for binaries with a random distribution of orbital elements that on average the true semi-major axis is about 1.3× larger than the projected semi-major axis.) To estimate the total system mass, we use the 36 pc distance inferred from the composite spectra fitting and the aforementioned $BC_K$ to estimate bolometric luminosities of $2.2 \times 10^{-5}$ and $1.2 \times 10^{-5}$ $L_\odot$ for the two components. Models by Burrows et al. (2001) give total masses for the system of about 60 $M_{Jup}$, 85 $M_{Jup}$, and 145 $M_{Jup}$ for assumed ages of 0.5, 1.0, and 5.0 Gyr. For an assumed semi-major axis of 4.0 AU, these mass estimates lead to an expected orbital period of 22–33 years. More generally, Torres (1999) shows that ≈85% of randomly oriented orbits have a true semi-major axis of 0.5–2.0× the projected separation, corresponding to a range of orbital periods of ≈8–95 yr for SDSS J1534+1615AB.

## 4. Discussion

### 4.1. The Nature of the L/T Transition

The rapid changes in near-IR colors at the L/T transition are generally understood to be due to a change in the photospheric dust content, but the very abrupt nature of this effect over a small inferred range in effective temperature remains a challenge to theoretical models. One key observational characteristic of the L/T transition is the unusual strong (∼1 mag) brightening of the $J$-band flux among the early and mid-T dwarfs compared to the late-L dwarfs (Dahn et al. 2002; Tinney et al. 2003; Vrba et al. 2004). This brightening is also seen at far-red ($I$ and $Z$) and other near-IR wavelengths ($H$ and $K$), though the effect is greatest at $J$-band. This wavelength dependence is expected, since at $J$-band the photospheric opacities are most sensitive to the properties of the clouds (Burrows et al. 2006).

Models can qualitatively accomodate the observed transition from the very red L dwarfs to the very blue T dwarfs (Marley et al. 2002; Tsuji 2002; Burrows et al. 2006). But no model thus far has succcessfully reproduced the observed $J$-band brightening along a single evolutionary track. Based on a suggestion by Ackerman & Marley (2001), Burgasser et al. (2002a) show that disruption of the condensate clouds at fixed $T_{\rm eff}$ could produce an enhancement of the $J$-band flux, as holes in the cloud deck reveal the deeper, hotter regions of the photosphere. Knapp et al. (2004) speculate that a rapid increase in the dust sedimentation efficiency over a small range of $T_{\rm eff}$ could be responsible. However, as pointed out by Burrows et al. (2006), these explanations are ad hoc, lacking a firm physical basis for the rapid transition.

A very different picture is suggested by Tsuji & Nakajima (2003). They propose that the $J$-band brightening does not occur along the evolutionary track of a given object. Rather, in their "unified cloudy model" the $T_{\rm eff}$ at which the L dwarf sequence merges with the T dwarf sequence depends on surface gravity: for younger or lower-mass objects, the L/T transition occurs at younger

ages and brighter $J$-band absolute magnitudes than for older or higher-mass objects. Thus, in their models the $J$-band brightening arises from the mass and age spreads within the known ensemble of L and T dwarfs and does not occur during the evolution of a single object. Objects that comprise the $J$-band brightening are predicted to be younger and to have lower surface gravities than objects which do not (c.f. Tinney et al. 2003).

The flux crossover in the near-IR that we observe in SDSS J1534+1615AB provides a benchmark for understanding the $J$-band brightening, as the binary presumably constitutes a system of common age and metallicity and nearly identical surface gravity. This crossover cannot be explained by the aforementioned unified cloudy model of Tsuji & Nakajima (2003). Their model isochrones show that no $J$-band brightening occurs for a coeval population, in disagreement with our observations of SDSS J1534+1615AB. The fact that SDSS J1534+1615AB displays the $J$-band brightening between its two coeval components reveals that the phenomenon can originate from processes intrinsic to ultracool photospheres with very similar surface gravities, such as the aforementioned cloud disruption and/or rapid dust settling scenarios.[4] Similarly, models by Burrows et al. (2006) indicate that variations in metallicities among the observed L and T dwarfs could be responsible for the $J$-band brightening (though this is not the preferred solution of Burrows et al.). SDSS J1534+1615AB demonstrates that objects of the same metallicity can exhibit the $J$-band brightening.

A good point of comparison is the T dwarf binary $\epsilon$ Ind Bab (McCaughrean et al. 2004). Scholz et al. (2003) determined an integrated-light spectral type of approximately T2.5 using the Geballe et al. (2002) classification scheme; we analyzed the published spectrum and found that the type is unchanged with the newer Burgasser et al. (2005a) scheme. The individual components of this $0.7''$ (2.6 AU) binary have spectral types of T1 and T6 on the Burgasser et al. scheme. The near-IR colors are consistent with $\epsilon$ Ind Ba having a comparable spectral type to SDSS J1534+1615A and $\epsilon$ Ind Bb being about one subclass later than SDSS J1534+1615B (Figure 2).[5] However, the flux ratios of $\epsilon$ Ind Bab do not show the crossover seen between the T1.5 ad T5.5 components of SDSS J1534+1615AB. This suggests that by spectral type T6 the $J$-band brightening no longer occurs, consistent with the observed CMD of T dwarfs (and ignoring possible complications due to surface gravity effects, as the $\epsilon$ Ind system is somewhat younger [1–2 Gyr] than expected for field objects).

---

[4]The reappearance of KI and FeH absorption in the far-red spectra of T2–T5 dwarfs, after having weakened among the late-L dwarfs (Burgasser et al. 2002a; Nakajima et al. 2004; Cushing et al. 2005), also argues that true photospheric processes are involved in the $J$-band brightening.

[5]We recomputed photometry for the individual components of $\epsilon$ Ind Bab. The McCaughrean et al. (2004) determination assumed that the VLT/NACO and 2MASS filter systems were identical. Based on synthetic photometry, we determined the (small) color terms between the two filter systems specific for T dwarfs and then used the published measurements to re-compute the colors: $(J-H)_{MKO} = \{0.53, -0.34\}$, $(H-K)_{MKO} = \{0.18, -0.34\}$, and $(J-K)_{MKO} = \{0.71, -0.69\}$ for components A and B, respectively. The resulting colors are $\leq$0.03 mags different from the published values.

### 4.2. Is the $J$-Band Brightening Enhanced by Unrecognized Binarity?

The flux crossover seen in the near-IR for SDSS J1534+1615AB demonstrates that the $J$-band brightening is a true physical effect and not solely a manifestation of large physical variations among the L and T dwarfs with known distances (unless SDSS J1534+1615B itself is an unresolved binary). However, the integrated-light photometry of SDSS J1534+1615 is in accord with the other $J$-band brightening objects (Figures 2, 4, and 5), most of which have not yet been imaged at high angular resolution.[6] This suggests that unrecognized binarity among early/mid-T dwarfs may strongly affect the appearance of the $J$-band brightening in the brown dwarf CMD. Furthermore, Burgasser et al. (2006) have recently noted that objects with spectral types of L7–T2 appear to have a higher binary frequency relative to earlier-type L dwarfs and mid/late-type T dwarfs (though a complete analysis of the selection biases is still needed). This finding covers an earlier spectral type range than the $J$-band brightening objects, but it does provide more evidence that binarity likely plays an important role in the L/T transition.

To examine this notion further, we consider here a scenario in which truly single $J$-band brightening objects are in fact rare. In this situation, it is the blended light of two components with different spectral types that produces an integrated-light spectral type of ≈T2–T4.5. Thus, the binary frequency of these spectral subclasses is greater compared to other T dwarfs, and the apparent amplitude of the $J$-band brightening effect is enhanced. Vrba et al. (2004) suggested that the $J$-band brightening cannot be due to unresolved binarity, because a significant number of objects contribute to the effect. However, their implicit assumption is that a given spectral subclass contains a mix of singles and binaries. Their objection would not be relevant in our scenario, wherein the reason that most objects are classified as T2–T4.5 is because they are binaries.

The observed CMD of T dwarfs lends some support to the idea that binarity might enhance the amplitude of the $J$-band brightening. Unrecognized binarity can add up to 0.75 mag of scatter in the absolute magnitudes, in addition to scatter caused by other effects, e.g., variations in surface gravity (Knapp et al. 2004; Burrows et al. 2006). Therefore, we would naturally expect at least this much scatter in the absolute magnitudes at a given spectral subclass, and this is largely observed (e.g., Figure 4 in this paper; Figure 2 of Vrba et al. 2004; Figure 9 of Tinney et al. 2003; Figure 8 of Knapp et al. 2004). However, the $J$-band brightening objects appear to have a *smaller* scatter in their absolute magnitudes compared to earlier and later spectral subclasses. This reduced scatter could be explained if in fact most $J$-band brightening objects are binaries, with truly single objects being rare. (An alternative explanation would be that the reduced scatter arises from a selection effect in the targets chosen by the parallax programs. However, it is not obvious what effect would act only on the $J$-band brightening objects and not the other subclasses.)

A similar hint, in a slightly different form, is seen in the effective temperatures of L and

[6]Likewise, the integrated-light spectrum of SDSS J1534+1615 shows no strong differences from the spectra of the other two known T3.5 objects, SDSS J1750+1759 (Geballe et al. 2002) and SDSS J1214+6316 (Chiu et al. 2006).

T dwarfs derived by Golimowski et al. (2004a). Their results suggest that T2–T4.5 dwarfs may have slightly higher temperatures than the late-L and T0–T1 dwarfs (see their Figure 6). While this discrepancy is within the uncertainties in the age estimates (which impact the model-derived radii used in the $T_{\rm eff}$ calculation), the systematically higher $T_{\rm eff}$'s are a curious trend in the data, especially under the assumption that the spectral type scale is a proxy for the $T_{\rm eff}$ scale (c.f. Tsuji 2005). One possibility would be that the T2–T4.5 dwarfs in Golimowski et al. have systematically younger ages than the earlier or later-type objects, but again it is not obvious how such a selection bias would occur. A more natural explanation is that the elevated $T_{\rm eff}$'s result from unrecognized binarity. This is amply demonstrated by the L3 dwarf Kelu-1 and the T0 dwarf SDSS J0423−0414 — their effective temperatures appear to to be anomalously large compared to objects of similar spectral types, but these deviations are in fact an artifact of previously unrecognized binarity (Liu & Leggett 2005; Burgasser et al. 2006). For the case of equal-luminosity components, $T_{\rm eff}$ will be overestimated by about 20% ($2^{1/4}$); applying this correction to the Golimowski et al. T2–T4.5 dwarfs would bring their temperatures into agreement with the earlier-type objects.[7]

In fact, if all the L and T dwarfs with anomolously high temperatures in the Golimowski et al. sample are actually unresolved binaries, we would infer that the $J$-band absolute magnitudes across the L/T transition are relatively constant (Figure 4). Similarly, the inflections in the brown dwarf CMDs at other wavelengths would also be impacted. Accounting for the possible binaries, Figure 5 shows that the apparent plateau in the $H$ and $K$-band fluxes of the early/mid-T dwarfs may be lessened, leading to a more monotonic dependence on on the spectral type. Table 3 provides polynomial fits for the absolute magnitude as a function of spectral type, with and without the possible binaries.

At face value, a higher binary frequency among the ≈T2–T4.5 objects relative to earlier and later-type objects may seem physically implausible. However, the binary frequency as a function of spectral type is not the same as the frequency as a function of $T_{\rm eff}$. While the frequency as a function of $T_{\rm eff}$ is expected to change smoothly, the frequency as a function of spectral type may not show the same behavior, since it also depends on how the light of individual binary components blends together. In particular, the large changes in spectral morphology and the non-monotonic behavior of the absolute magnitudes during the L/T transition may lead to interesting observational consequences when these objects form binaries.[8] For the sake of illustration, if we consider an

[7]By the same rationale, SDSS J0032+1410 (L8) and 2MASS J0328+2302 (L9.5) are candidates for being unresolved binaries based on their relatively high $T_{\rm eff}$'s.

[8]Since the IR absolute magnitudes around the L/T transition do not decrease monotonically as a function of spectral type, unresolved binaries in the L/T transition region with a range of mass ratios can be significantly displaced in the CMD in both absolute magnitude and integrated-light spectral type compared to the individual components. In contrast, if the magnitude-spectral type relation were monotonic and very steep, then a population of unresolved binaries would mostly lead to a spread in the magnitudes, due to the equal-mass binaries; the unequal-mass binaries would not have much impact on the CMD, since the secondary components would not substantially contribute to the integrated-light properties.

extreme example where truly single T2–T4.5 objects do not exist at all, the SDSS J1534+1615AB (T3.5) and $\epsilon$ Ind Bab (T2.5) systems demonstrate that these subclasses can be populated with binaries composed of an early and a late-type T dwarf – in this case, the T2–T4.5 dwarfs would have a 100% binary fraction, even if the earlier and later-type T dwarfs have much lower binary fractions.

A relative paucity of single objects in the $J$-band brightening regime can be naturally explained if the corresponding $T_{\rm eff}$ range is very small, e.g., as suggested by Kirkpatrick et al. (2000) and indicated by measurements from Vrba et al. (2004) and Golimowski et al. (2004a). The small $T_{\rm eff}$ range would correspond to a relatively short-lived evolutionary phase, and therefore relatively few substellar objects would be found in the corresponding spectral subclasses. However, even if truly single ≈T2–T4.5 objects are rare, a higher binary frequency among these objects may not be apparent in the spectral type distribution of objects found by 2MASS and SDSS. In such magnitude-limited surveys, the effective detection volume for binary stars is larger than for single stars, and thus a survey's observed spectral type distribution depends on several factors — the true binary frequency, the slope of the relationship between absolute magnitude and spectral type, and the effect of unresolved binarity on spectral types determined from integrated-light photometry and/or spectroscopy. A Monte Carlo simulation, beyond the scope of this paper, would be valuable in understanding the interplay of these effects.

Given that only six T2–T4.5 dwarfs have measured distances, the discussion here is inevitably speculative — such a small sample hinders more detailed considerations.[9] Similarly, our adopted spectral range of ≈T2–T4.5 for the strong $J$-band brightening phenomenon should be considered as approximate. The T dwarf binaries SDSS J1534+1615AB, $\epsilon$ Ind Bab, and SDSS J0423−0414AB all have components with estimated spectral types of T1–T2. Unless these components are themselves binary, this shows that single early-T dwarfs are not uncommon. Indeed the positions of these components in brown dwarf CMDs are quite similar (Figures 4 and 5) and are somewhat fainter than the T2 dwarf SDSS J1254−0122, which thus far appears to be a single object (Burgasser et al. 2003b).

If binarity does play a significant role in the $J$-band brightening objects, there are some natural consequences. (1) More extensive imaging surveys with *HST* and LGS AO should find a greater binary frequency among these objects compared to earlier and later-type objects, after accounting for selection effects inherent in current magnitude-limited samples of brown dwarfs. Of course, some systems may have projected separations below the resolution limit of imaging surveys and would

[9]The six T2–T4.5 dwarfs with known distances are SDSS J1254−0122 (T2), $\epsilon$ Ind Bab (T2.5 in integrated light), SDSS J1021−0304 (T3), SDSS J1750+1759 (T3.5), 2MASS J0559−1404 (T4.5), and SDSS J0207+0000 (T4.5) — see compilation in Burgasser et al. (2005a). Also, SDSS J0423−0414 (T0 in near-IR integrated light) has recently been resolved into a binary by Burgasser et al. (2006); the components have estimated spectral types of L6±1 and T2±1 based on their near-IR fluxes and modeling of the combined-light spectrum. Resolved $JHK$ magnitudes are not available for this system, so we estimate them for Figures 4 and 5 by scaling template spectra of the individual components to the resolved optical fluxes.

only be detectable as spectroscopic binaries (e.g. Maxted & Jeffries 2005). (2) Such binaries should often be composed of an earlier-type object, say late-L to early-T, and an object of approximately T5 or later. (3) More generally, the $J$-band brightening objects should have relatively lower space densities compared to other ultracool dwarfs. In this regard, a populous volume-limited sample of L and T dwarfs with trigonometric parallaxes would be valuable for studying the nature of the L/T transition. Such a sample is unlikely to be achieved with current parallax programs, which can only target a limited number of pre-selected objects. The upcoming Pan-STARRS project (Kaiser et al. 2002) will monitor the entire sky observable from Hawai'i with high astrometric precision (planned 1-d RMS astrometric error of 10 mas per observing epoch). The resulting dataset should be a promising means to assemble a large sample of brown dwarfs with accurate distances.

## 5. Summary

We have obtained high angular resolution imaging of the T3.5 dwarf SDSS J1534+1615 using the Keck sodium LGS AO system. SDSS J1534+1615 is resolved into a 0.11″ binary, and its low proper motion and distinctive optical/IR colors indicate that it is a physical pair. The resolved near-IR colors give estimated spectral types of T1.5±0.5 and T5.5±0.5, consistent with modeling the integrated-light spectrum as the blend of two components. This analysis also produces an estimated distance of 36 pc, based on the distances to the mid-T dwarfs used in the modeling. The inferred (distance-independent) differences in the masses and surface gravities of the two components are about 20% and 0.1 dex, respectively.

SDSS J1534+1615AB serves as a new benchmark for understanding the $J$-band brightening seen among the early/mid-T dwarfs. The binary's near-IR flux ratios show an inversion, wherein component A is brighter at $H$ and $K$-bands but component B is brighter at $J$-band by about 0.2 mags. Thus, this binary system embodies the $J$-band brightening phenomenon seen in the CMD of T dwarfs. Since the components of SDSS J1534+1615 presumably have a common age, a common metallicity, and a very similar surface gravity, our results demonstrate that the $J$-band brightening is intrinsic to ultracool photospheres and not necessarily a by-product of observing an ensemble of brown dwarfs with different masses, ages, and/or metallicities. Likewise, the brightening mechanism must be able to operate over a relatively small range (≈200 K) in effective temperature. The magnitudes and colors of SDSS J1534+1615AB and the binary T dwarf $\epsilon$ Ind Bab are quite similar. However, $\epsilon$ Ind Bab, with resolved spectral types of T1 and T6, does not show a crossover in its near-IR flux ratios, suggesting that the $J$-band brightening may end by around spectral type T5.

Based on the limited observations to date, we have considered the possibility that the large amplitude of the $J$-band brightening among early/mid-T dwarfs is caused by a high frequency of unresolved binaries. SDSS J1534+1615AB and $\epsilon$ Ind Bab provide examples of objects which appear to reside at/near the CMD location of the $J$-band brightening, but once their resolved properties are taken into account, the individual components are consistent with early-T's and mid/late-T's. We speculate that the possibly smaller scatter seen in the infrared CMDs and the slightly higher $T_{\rm eff}$'s

inferred for the ≈T2–T4.5 dwarfs could be hints of unresolved binarity, leading to an enhancement in the apparent amplitude of the $J$-band brightening. In this interpretation, truly single ≈T2–T4.5 objects would be relatively rare, with most objects of these spectral subclasses being composed of the blended light of an earlier and later-type component. This hypothesis is in accord with the small $T_{\rm eff}$ range inferred for the late-L to mid-T subclasses; photospheric dust removal seems to occur very rapidly during the L/T transition.

Further study of SDSS J1534+1615AB will shed light on the nature of the L/T transition and the $J$-band brightening. A trigonometric parallax will accurately determine the CMD positions of the combined system and individual components. Resolved spectroscopy of the two components will allow for more accurate spectral classification. Also, given the common metallicity and similar surface gravities of the two components, such data can isolate the temperature-sensitive and dust-sensitive features in the spectra of the early/mid-T dwarfs. Given the estimated ∼28 yr period, follow-up high angular resolution imaging over the next several years can trace a significant fraction of the orbital motion and lead to a dynamical mass estimate. Ultimately, a much larger sample of T dwarf binaries from *HST*, LGS AO, and IR radial velocities will provide the means to fully explore the physical processes encapsulated in the substellar color-magnitude diagram.

We gratefully acknowledge the Keck LGS AO team for their impressive efforts in bringing the LGS AO system to fruition. It is a pleasure to thank Antonin Bouchez, David LeMignant, Marcos van Dam, Randy Campbell, Robert LaFon, Gary Punawai, Peter Wizinowich, and the Keck Observatory staff for assistance with the observations; John Rayner, Robert Jedicke, Adam Burrows, Adam Burgasser, Neill Reid, and Marcos van Dam for productive discussions; and Dagny Looper for a careful reading of the manuscript. We thank Alan Stockton for a fortuitous swap of observing nights. Our research has benefitted from the 2MASS data products; NASA's Astrophysical Data System; the SIMBAD database operated at CDS, Strasbourg, France; and the M, L, and T dwarf compendium housed at DwarfArchives.org and maintained by Chris Gelino, Davy Kirkpatrick, and Adam Burgasser (Kirkpatrick 2003; Gelino et al. 2004). ML acknowledges support for this work from NSF grant AST-0507833 and a Sloan Research Fellowship. XF is supported by NSF grant AST-0307384, a Sloan Research Fellowship, and a Packard Fellowship for Science and Engineering. Funding for the SDSS and SDSS-II has been provided by the Alfred P. Sloan Foundation, the Participating Institutions, the National Science Foundation, the U.S. Department of Energy, the National Aeronautics and Space Administration, the Japanese Monbukagakusho, the Max Planck Society, and the Higher Education Funding Council for England. The SDSS Web Site is http://www.sdss.org/. The SDSS is managed by the Astrophysical Research Consortium for the Participating Institutions. The Participating Institutions are the American Museum of Natural History, Astrophysical Institute Potsdam, University of Basel, Cambridge University, Case Western Reserve University, University of Chicago, Drexel University, Fermilab, the Institute for Advanced Study, the Japan Participation Group, Johns Hopkins University, the Joint Institute for Nuclear Astrophysics, the Kavli Institute for Particle Astrophysics and Cosmology, the Korean Scientist Group, the Chinese Academy of Sciences (LAMOST), Los Alamos National Laboratory, the Max-

Planck-Institute for Astronomy (MPIA), the Max-Planck-Institute for Astrophysics (MPA), New Mexico State University, Ohio State University, University of Pittsburgh, University of Portsmouth, Princeton University, the United States Naval Observatory, and the University of Washington. Finally, the authors wish to recognize and acknowledge the very significant cultural role and reverence that the summit of Mauna Kea has always had within the indigenous Hawaiian community. We are most fortunate to have the opportunity to conduct observations from this mountain.

## REFERENCES

Ackerman, A. S. & Marley, M. S. 2001, ApJ, 556, 872

Baraffe, I., Chabrier, G., Barman, T. S., Allard, F., & Hauschildt, P. H. 2003, A&A, 402, 701

Becklin, E. E. & Zuckerman, B. 1988, Nature, 336, 656

Bouchez, A. H. et al. 2004, in Advancements in Adaptive Optics. Edited by Domenico B. Calia, Brent L. Ellerbroek, and Roberto Ragazzoni. Proceedings of the SPIE., Vol. 5490, 321–330

Bouy, H., Brandner, W., Martín, E. L., Delfosse, X., Allard, F., & Basri, G. 2003, AJ, 126, 1526

Burgasser, A. J., Geballe, T. R., Leggett, S. K., Kirkpatrick, J. D., & Golimowski, D. A. 2005a, ArXiv Astrophysics e-prints

Burgasser, A. J., Kirkpatrick, J. D., Liebert, J., & Burrows, A. 2003a, ApJ, 594, 510

Burgasser, A. J., Kirkpatrick, J. D., & Lowrance, P. J. 2005b, AJ, 129, 2849

Burgasser, A. J., Kirkpatrick, J. D., Reid, I. N., Brown, M. E., Miskey, C. L., & Gizis, J. E. 2003b, ApJ, 586, 512

Burgasser, A. J., Marley, M. S., Ackerman, A. S., Saumon, D., Lodders, K., Dahn, C. C., Harris, H. C., & Kirkpatrick, J. D. 2002a, ApJ, 571, L151

Burgasser, A. J., Reid, I. N., Leggett, S. K., Kirkpatrick, J. D., Liebert, J., & Burrows, A. 2006, ApJ, in press (arXiv:astro-ph/0510580)

Burgasser, A. J. et al. 2000, ApJ, 531, L57

—. 2002b, ApJ, 564, 421

Burrows, A., Hubbard, W. B., Lunine, J. I., & Liebert, J. 2001, Reviews of Modern Physics, 73, 719

Burrows, A., Sudarsky, D., & Hubeny, I. 2006, ApJ, in press (astro-ph/0509066)

Chiu, K. et al. 2006, ApJ, in press (astro-ph/0601089)

Cruz, K. L., Burgasser, A. J., Reid, I. N., & Liebert, J. 2004, ApJ, 604, L61

Cushing, M. C., Rayner, J. T., & Vacca, W. D. 2005, ApJ, 623, 1115

Dahn, C. C. et al. 2002, AJ, 124, 1170

Diolaiti, E., Bendinelli, O., Bonaccini, D., Close, L., Currie, D., & Parmeggiani, G. 2000, A&AS, 147, 335

Enoch, M. L., Brown, M. E., & Burgasser, A. J. 2003, AJ, 126, 1006

Fischer, D. A. & Marcy, G. W. 1992, ApJ, 396, 178

Freed, M., Close, L. M., & Siegler, N. 2003, ApJ, 584, 453

Geballe, T. et al. 2002, ApJ, 564, 466

Gelino, C. R., Kirkpatrick, J. D., & Burgasser, A. J. 2004, BAAS, 205

Gizis, J. E., Reid, I. N., Knapp, G. R., Liebert, J., Kirkpatrick, J. D., Koerner, D. W., & Burgasser, A. J. 2003, AJ, 125, 3302

Golimowski, D. A. et al. 2004a, AJ, 127, 3516

—. 2004b, AJ, 128, 1733

Kaiser, N. et al. 2002, in Survey and Other Telescope Technologies and Discoveries. Edited by Tyson, J. Anthony; Wolff, Sidney. Proceedings of the SPIE, Volume 4836, pp. 154-164 (2002)., 154–164

Kirkpatrick, J. D. 2003, in Proceedings of IAU Symposium 211: Brown Dwarfs, ed. E. Martin, 189

Kirkpatrick, J. D. 2005, ARA&A, 43, 195

Kirkpatrick, J. D., Dahn, C. C., Monet, D. G., Reid, I. N., Gizis, J. E., Liebert, J., & Burgasser, A. J. 2001, AJ, 121, 3235

Kirkpatrick, J. D., Reid, I. N., Liebert, J., Gizis, J. E., Burgasser, A. J., Monet, D. G., Dahn, C. C., Nelson, B., & Williams, R. J. 2000, AJ, 120, 447

Knapp, G. R. et al. 2004, AJ, 127, 3553

Koen, C., Matsunaga, N., & Menzies, J. 2004, MNRAS, 354, 466

Koen, C., Tanabé, T., Tamura, M., & Kusakabe, N. 2005, MNRAS, 362, 727

Koerner, D. W., Kirkpatrick, J. D., McElwain, M. W., & Bonaventura, N. R. 1999, ApJ, 526, L25

Leggett, S. K., Allard, F., Burgasser, A. J., Jones, H. R. A., Marley, M. S., & Tsuji, T. 2004, ArXiv Astrophysics e-prints

Leggett, S. K. et al. 2002, ApJ, 564, 452

Liu, M. C., Fischer, D. A., Graham, J. R., Lloyd, J. P., Marcy, G. W., & Butler, R. P. 2002, ApJ, 571, 519

Liu, M. C. & Leggett, S. K. 2005, ApJ, 634, 616

Marley, M. S., Seager, S., Saumon, D., Lodders, K., Ackerman, A. S., Freedman, R. S., & Fan, X. 2002, ApJ, 568, 335

Martín, E. L., Brandner, W., & Basri, G. 1999, Science, 283, 1718

Maxted, P. F. L. & Jeffries, R. D. 2005, MNRAS, 362, L45

McCaughrean, M. J., Close, L. M., Scholz, R.-D., Lenzen, R., Biller, B., Brandner, W., Hartung, M., & Lodieu, N. 2004, A&A, 413, 1029

Metchev, S. A. & Hillenbrand, L. A. 2004, ApJ, 617, 1330

Monet, D. G. et al. 2003, AJ, 125, 984

Nakajima, T., Oppenheimer, B. R., Kulkarni, S. R., Golimowski, D. A., Matthews, K., & Durrance, S. T. 1995, Nature, 378, 463

Nakajima, T., Tsuji, T., & Yanagisawa, K. 2001, ApJ, 561, L119

—. 2004, ApJ, 607, 499

Perryman, M. A. C. et al. 1997, A&A, 323, L49

Potter, D., Martín, E. L., Cushing, M. C., Baudoz, P., Brandner, W., Guyon, O., & Neuhäuser, R. 2002, ApJ, 567, L133

Rebolo, R., Zapatero Osorio, M. R., Madruga, S., Bejar, V. J. S., Arribas, S., & Licandro, J. 1998, Science, 282, 1309

Reid, I. N., Gizis, J. E., Kirkpatrick, J. D., & Koerner, D. W. 2001, AJ, 121, 489

Reid, I. N., Lewitus, E., Burgasser, A. J., & Cruz, K. L. 2006, ApJ, 639, 1114

Scholz, R.-D., McCaughrean, M. J., Lodieu, N., & Kuhlbrodt, B. 2003, A&A, 398, L29

Simons, D. A. & Tokunaga, A. 2002, PASP, 114, 169

Thorstensen, J. R. & Kirkpatrick, J. D. 2003, PASP, 115, 1207

Tinney, C. G., Burgasser, A. J., & Kirkpatrick, J. D. 2003, AJ, 126, 975

Tokunaga, A. T., Simons, D. A., & Vacca, W. D. 2002, PASP, 114, 180

Torres, G. 1999, PASP, 111, 169

Tsuji, T. 2002, ApJ, 575, 264

—. 2005, ApJ, 621, 1033

Tsuji, T. & Nakajima, T. 2003, ApJ, 585, L151

Vrba, F. J. et al. 2004, AJ, 127, 2948

Wizinowich, P. L. et al. 2004, in Advancements in Adaptive Optics. Edited by Domenico B. Calia, Brent L. Ellerbroek, and Roberto Ragazzoni. Proceedings of the SPIE., Vol. 5490, 1–11

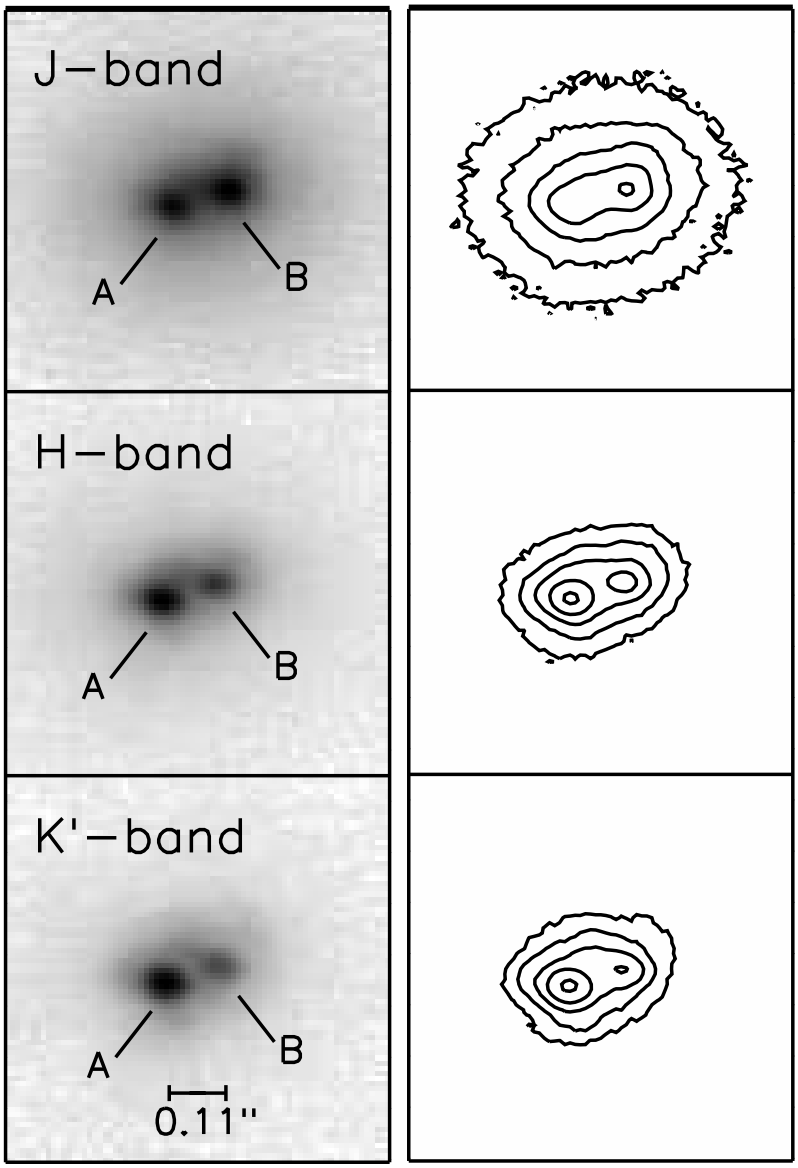


Fig. 1.— $JHK'$-band imaging of SDSS J1534+1615AB from Keck LGS AO. North is up and east is left. Each image is 0.75″ on a side. The binary separation is 0.110″ ± 0.005″. Contours are drawn from 90%, 45%, 22.5%, 11.2%, 5.6% and 2.8% of the peak value in each bandpass. The source to the southeast (left) is component A (brighter at $H$ and $K'$, fainter at $J$, spectral type T1.5±0.5), and the source to the northwest (right) is component B (fainter at $H$ and $K'$, brighter at $J$, spectral type T5.5±0.5). The images are slightly east-west elongated due to telescope windshake.

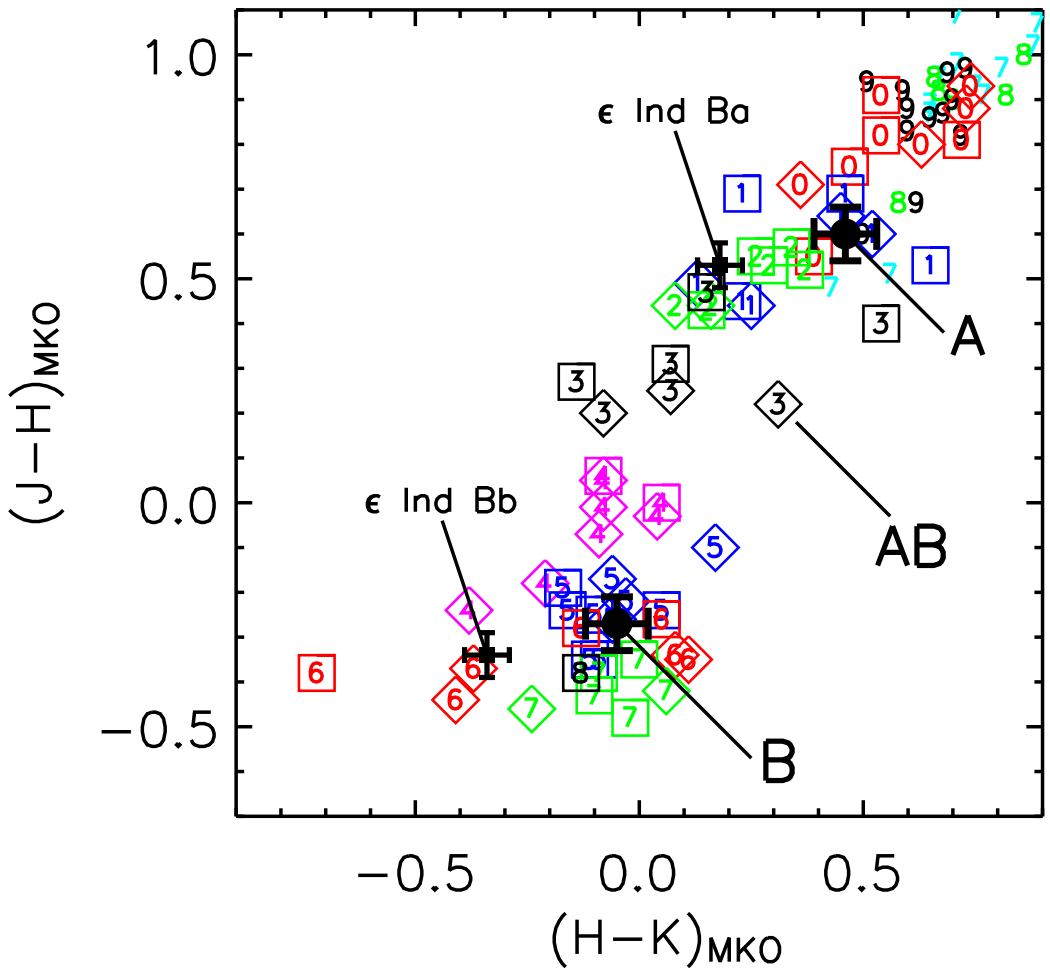


Fig. 2.— Near-IR colors of SDSS J1534+1615AB compared with nearby late-L and T dwarfs from Knapp et al. (2004) and Chiu et al. (2006). The numbers indicate the near-IR spectral subclass of the objects, with half subclasses being rounded down (e.g., T3.5 is labeled as "3"). The late-L dwarfs (classified on the Geballe et al. 2002 scheme) are plotted as bare numbers. The T dwarfs (on the Burgasser et al. 2005a scheme) are plotted as circumscribed numbers, with squares for integer subclasses (e.g., T3) and diamonds for half subclasses (e.g., T3.5). The photometry errors are comparable to or smaller than the size of the plotting symbols. Known binaries are excluded except for SDSS J1534+1615AB, which is labeled on the plot as A, B, and AB. The inferred spectral types for components A and B of SDSS J1534+1615 are T1.5±0.5 and T5.5±0.5, respectively. The individual components of $\epsilon$ Ind Bab are shown for comparison, where we have converted the published photometry to the MKO system (see § 4.1) and assumed errors of 0.05 mags.

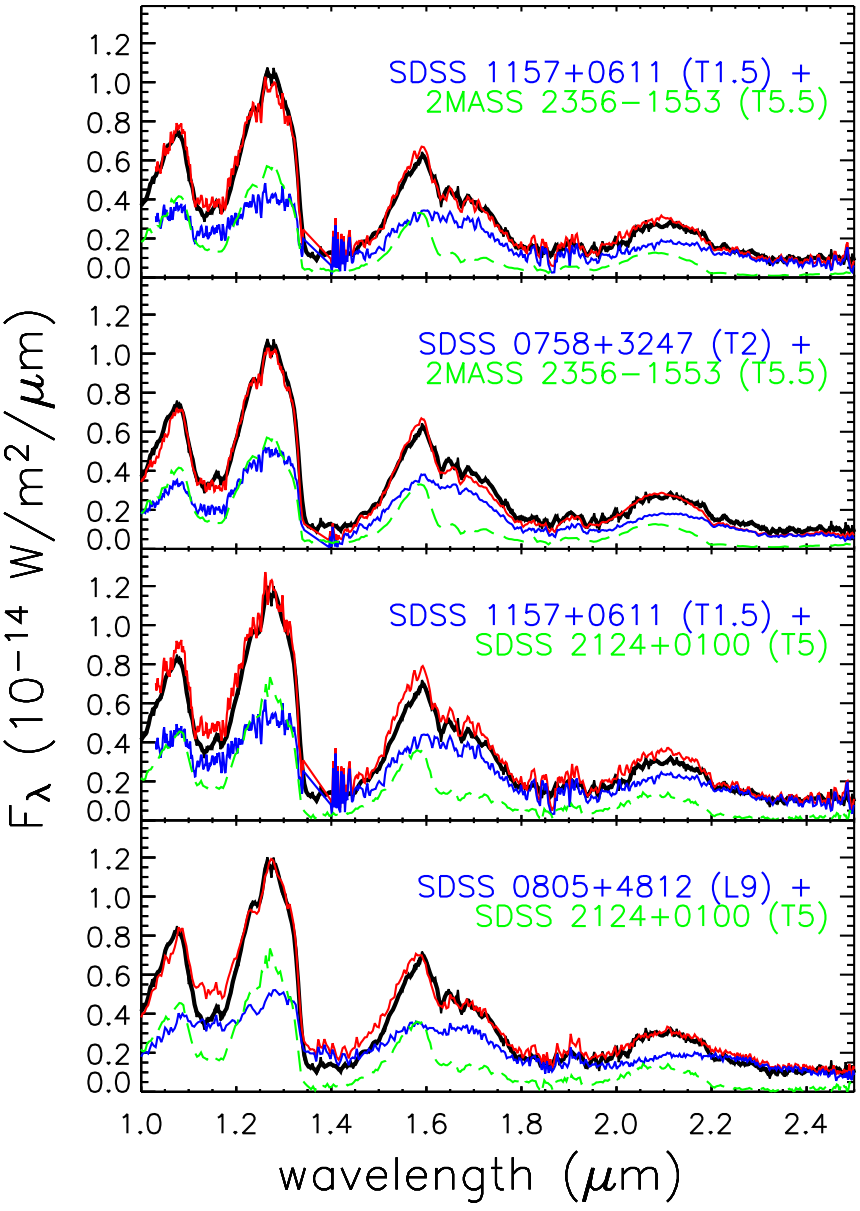


Fig. 3.— Results from modeling the integrated-light near-IR spectrum of SDSS J1534+1615 (black lines; Chiu et al. 2006) as the sum of two T dwarfs (red lines): one early-T template (blue solid lines) and one late-T template (green dashed lines). The template objects are chosen to have similar IR colors as the resolved components of SDSS J1534+1615AB, and the observed $J$-band flux ratio is used in scaling and combining the template spectra. The only free parameter in the fitting is the distance to SDSS J1534+1615AB. (See § 3 for details.) The agreement between the observed spectrum and the modeled blends is good, especially for the topmost panel, meaning that the spectral types inferred for SDSS J1534+1615A and B from the near-IR colors are consistent with the integrated-light spectrum. The bottommost panel shows the match attempted using a blue late-L dwarf as component A; the depth of the $J$-band water absorption is not well-matched. The template spectra are from Chiu et al. (2006), Knapp et al. (2004), and Burgasser et al. (2002b).

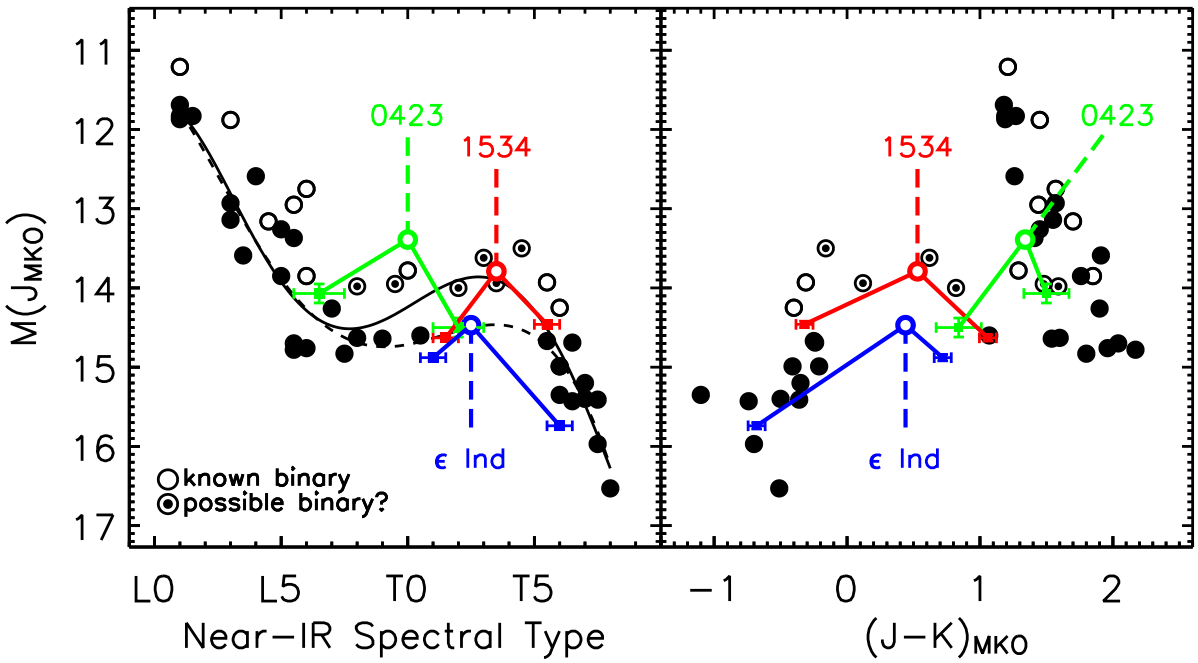


Fig. 4.— $J$-band absolute magnitude as a function of near-IR spectral type and $J-K$ color, based on data tabulated by Knapp et al. (2004) and excluding sources with S/N<4 parallax measurements (SDSS J1435−0043 [T6], SDSS J0207+0000 [T4.5], and SDSS J0837−0000 [T0.5]). Spectral types are based on the Geballe et al. (2002) scheme for the L dwarfs and the Burgasser et al. (2005a) scheme for the T dwarfs. The integrated-light properties of the binary T dwarfs SDSS J1534+1615AB, $\epsilon$ Ind Bab, and SDSS J0423−0414AB are plotted as colored open circles, and the colored filled squares show the individual components. (For the latter two objects, see § 4 for a description of their resolved measurements.) The distance to SDSS J1534+1615AB is based on modeling the integrated-light spectrum as the blend of two components (see § 3), and thus is more uncertain than the trigonometric distances for $\epsilon$ Ind Bab and SDSS J0423−0414AB. Errors in $M(J)$ are comparable to the symbol size. On the left, the solid line shows a 5th-order polynomial fit for $M(J)$ versus near-IR spectral type, excluding known binaries. To illustrate the potential significance of binarity, the dashed line shows the same order fit, excluding both known and possible binaries. Possible binaries were selected based on their relatively high $T_{\rm eff}$ compared to objects of similar spectral type in the Golimowski et al. (2004a) measurements (see § 4.2); these are SDSS J0032+1410 (L8), 2MASS J0328+2302 (L9.5), SDSS J1254−0122 (T2), SDSS J1021−0304 (T3), SDSS J1750+1759 (T3.5), and 2MASS J0559−1404 (T4.5). Table 3 provides the coefficients of the polynomial fits.

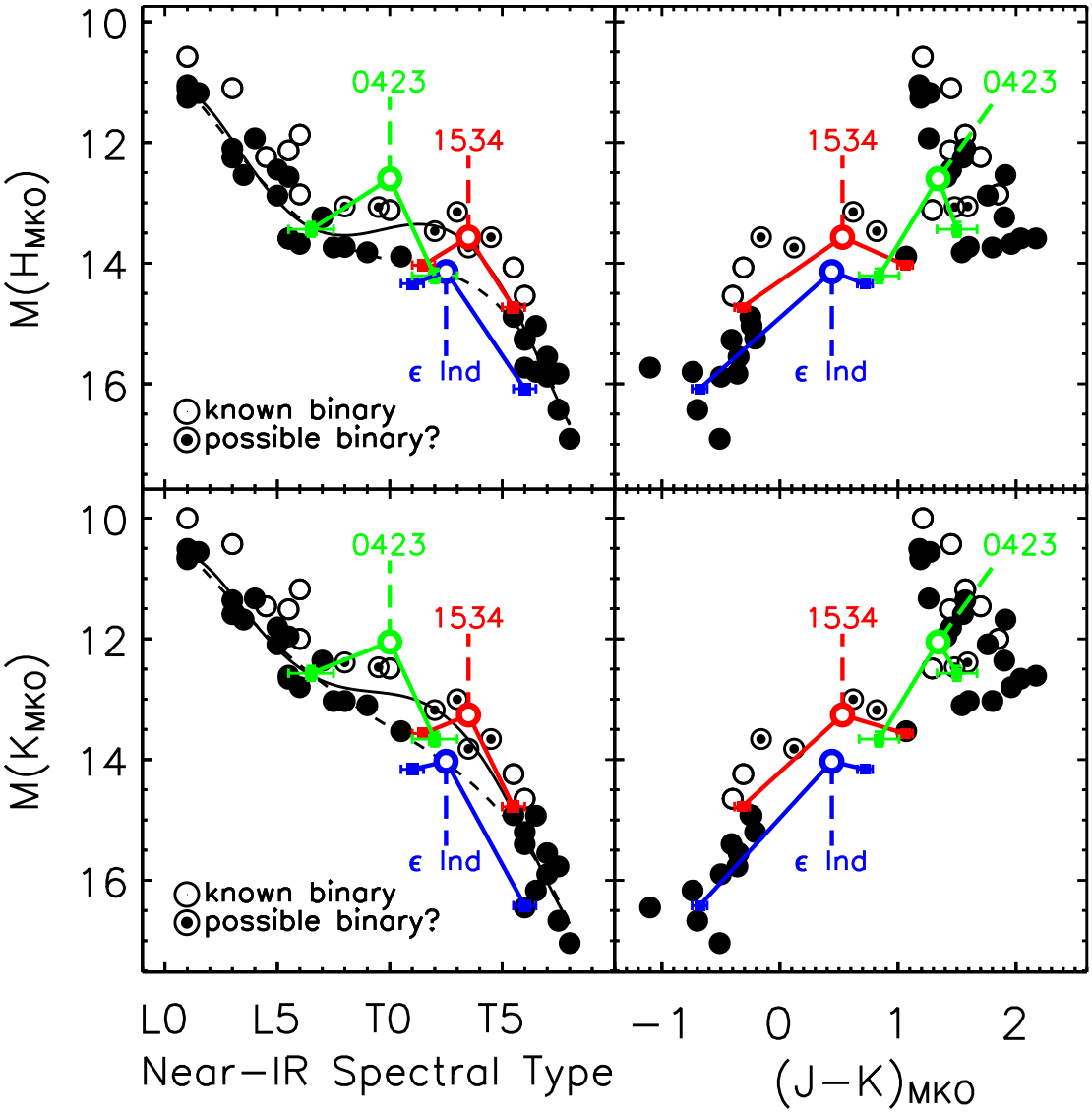


Fig. 5.— $H$ and $K$-band absolute magnitudes as a function of near-IR spectral type and $J - K$ color. See Figure 4 for a description of the content.

Table 1. SDSS J1534+1615AB Binary Properties[a]

| Property | Measurement |
|---|---|
| Separation (mas) | 110 ± 5 |
| Position angle (deg) | 287.6 ± 1.3 |
| $\Delta J$ (mags) | −0.17 ± 0.04 |
| $\Delta H$ (mags) | 0.70 ± 0.04 |
| $\Delta K'$ (mags) | 1.07 ± 0.05 |
| Proper motion: $\mu_\alpha$, $\mu_\delta$ (mas yr$^{-1}$) | −142 ± 14, −57 ± 10 |
| Mass ratio $M_B/M_A$ | 0.80 ± 0.05 |
| Luminosity ratio $\log(L_A/L_B)$ (dex) | 0.3 ± 0.1 |
| Surface gravity ratio $\log(g_A/g_B)$ (dex) | 0.10 ± 0.05 |
| Estimated distance (pc) | ≈36 |
| Total mass ($M_{Jup}$): 0.5, 1.0, 5.0 Gyr | 60, 85, 145 |
| Estimated orbital period (yr) | 22–33 |

[a]All photometry on the MKO system.

Table 2. Resolved Properties of SDSS J1534+1615AB[a]

| Property | SDSS J1534+1615A | SDSS J1534+1615B |
|---|---|---|
| $J$ (mags) | 17.43 ± 0.04 | 17.26 ± 0.04 |
| $H$ (mags) | 16.83 ± 0.04 | 17.53 ± 0.04 |
| $K$ (mags) | 16.37 ± 0.06 | 17.58 ± 0.06 |
| $J - H$ (mags) | 0.60 ± 0.06 | −0.27 ± 0.06 |
| $H - K$ (mags) | 0.46 ± 0.07 | −0.05 ± 0.07 |
| $J - K$ (mags) | 1.06 ± 0.07 | −0.32 ± 0.07 |
| Estimated spectral type[b] | T1.5 ± 0.5 | T5.5 ± 0.5 |

[a]All photometry on the MKO photometric system.

[b]Based on the Burgasser et al. (2005a) classification scheme.

Table 3. Coefficients of Polynomial Fits to Absolute Magnitudes versus Near-IR Spectral Type

| Magnitude | $c_0$ | $c_1$ | $c_2$ | $c_3$ | $c_4$ | $c_5$ | RMS |
|---|---|---|---|---|---|---|---|
| Excluding Known Binaries | | | | | | | |
| $M(J_{MKO})$ | 11.746 | −2.259e−1 | 3.229e−1 | −5.155e−2 | 2.966e−3 | −5.648e−5 | 0.39 |
| $M(H_{MKO})$ | 11.263 | −4.164e−1 | 3.565e−1 | −5.610e−2 | 3.349e−3 | −6.720e−5 | 0.35 |
| $M(K_{MKO})$ | 10.731 | −3.964e−1 | 3.150e−1 | −4.912e−2 | 2.994e−3 | −6.179e−5 | 0.39 |
| Excluding Known and Possible Binaries | | | | | | | |
| $M(J_{MKO})$ | 11.359 | 3.174e−1 | 1.102e−1 | −1.877e−2 | 9.169e−4 | −1.233e−5 | 0.37 |
| $M(H_{MKO})$ | 10.767 | 2.744e−1 | 8.955e−2 | −1.552e−2 | 8.319e−4 | −1.315e−5 | 0.30 |
| $M(K_{MKO})$ | 10.182 | 3.688e−1 | 2.028e−2 | −4.488e−3 | 2.301e−4 | −2.466e−6 | 0.34 |

Note. — These are the coefficients of the 5th-order polynomial fits plotted in Figures 4 and 5 for the IR absolute magnitudes as a function of near-IR spectral type. The fits are defined as

$$Magnitude = \sum_{i=0}^{5} c_i \times (SpT)^i$$

where the numerical spectral type is defined as $SpT = 1$ for L1, $SpT = 2$ for L2, $SpT = 10$ for T0, etc. The L dwarfs are classified on the Geballe et al. (2002) scheme and the T dwarfs on the Burgasser et al. (2005a) scheme. The fits are applicable from L1 to T8. Possible binaries were selected based on their relatively high $T_{\rm eff}$ compared to objects of similar spectral type — see § 4.2 and the caption of Figure 4. The last column gives the standard deviation about the fit in magnitudes.